

Knowledge Transfer Between Artificial Intelligence Systems

Ivan Yu. Tyukin^{a,b,c,*}, Alexander N. Gorban^{a,c}, Konstantin I. Sofeikov^{a,d}, Ilya Romanenko^d

^a*University of Leicester, Department of Mathematics, University Road, Leicester, LE1 7RH, UK*

^b*Department of Automation and Control Processes, St. Petersburg State University of Electrical Engineering, Prof. Popova str. 5, Saint-Petersburg, 197376, Russian Federation*

^c*UnivAI Ltd, 5 Park Court, Pyrford Road, West Byfleet, KT14 6SD, UK*

^d*Imaging and Vision Group, ARM Ltd, 1 Summerpool Rd, Loughborough, LE11 5RD, UK*

Abstract

We consider the fundamental question: how a legacy “student” Artificial Intelligent (AI) system could learn from a legacy “teacher” AI system or a human expert without complete re-training and, most importantly, without requiring significant computational resources. Here “learning” is understood as an ability of one system to mimic responses of the other and vice-versa. We call such learning an Artificial Intelligence knowledge transfer. We show that if internal variables of the “student” Artificial Intelligent system have the structure of an n -dimensional topological vector space and n is sufficiently high then, with probability close to one, the required knowledge transfer can be implemented by simple cascades of linear functionals. In particular, for n sufficiently large, with probability close to one, the “student” system can successfully and non-iteratively learn $k \ll n$ new examples from the “teacher” (or correct the same number of mistakes) at the cost of two additional inner products. The concept is illustrated with an example of knowledge transfer from a pre-trained convolutional neural network to a simple linear classifier with HOG features.

Keywords: Learning, neural networks, approximation, measure concentration

1. Introduction

Knowledge transfer between Artificial Intelligent systems has been the subject of extensive discussion in the literature for more than two decades [1], [2], [3], [4]. State-of-the art approach to date is to use, or salvage, parts of the

*Corresponding author

Email addresses: I.Tyukin@le.ac.uk (Ivan Yu. Tyukin), ag153@le.ac.uk (Alexander N. Gorban), sofeykov@gmail.com (Konstantin I. Sofeikov), Ilya.Romanenko@arm.com (Ilya Romanenko)

teacher AI system in the student AI followed by re-training of the student [5], [6]. Alternatives to AI salvaging include model compression [7], knowledge *distillation* [8], and *privileged information* [9]. These approaches demonstrated substantial success in improving generalization capabilities of AIs as well as in reducing computational overheads [10], in cases of knowledge transfer from larger AI to the smaller one. Notwithstanding, however, which of the above strategies is followed, their implementation often requires either significant resources including large training sets and power needed for training, or access to privileged information that may not necessarily be available to end-users. Thus new frameworks and approaches are needed.

In this contribution we provide new framework for automated, fast, and non-destructive process of knowledge spreading across AI systems of varying architectures. In this framework, knowledge transfer is accomplished by means of Knowledge Transfer Units comprising of mere linear functionals and/or their small cascades. Main mathematical ideas are rooted in measure concentration [11], [12], [13], [14], [15] and stochastic separation theorems [16] revealing peculiar properties of random sets in high dimensions. We generalize some of the latter results here and show how these generalizations can be employed to build simple one-shot Knowledge Transfer algorithms between heterogeneous AI systems whose state may be represented by elements of linear vector space of sufficiently high dimension. Once knowledge has been transferred from one AI to another, the approach also allows to “unlearn” new knowledge without the need to store a complete copy of the “student” AI is created prior to learning. We expect that the proposed framework may pave way for fully functional new phenomenon – Nursery of AI systems in which AIs quickly learn from each other whilst keeping their pre-existing skills largely intact.

The paper is organized as follows. Section 2 contains mathematical background needed to justify the proposed knowledge transfer algorithms. In Section 3 we present two algorithms for transferring knowledge between a pair of AI systems in which one operates as a teacher and the other functions as a student. Section 4 illustrates the approach with examples, and Section 5 concludes the paper.

2. Mathematical background

Let the set

$$\mathcal{M} = \{\mathbf{x}_1, \dots, \mathbf{x}_M\}$$

be an i.i.d. sample from a distribution in \mathbb{R}^n . Pick another set

$$\mathcal{Y} = \{\mathbf{x}_{M+1}, \dots, \mathbf{x}_{M+k}\}$$

from the same distribution at random. What is the probability that there is a linear functional separating \mathcal{Y} from \mathcal{M} ?

Below we provide three k -tuple separation theorems: for an equidistribution in $B_n(1)$ (Theorem 1 and 2) and for a product probability measure with bounded support (Theorem 3). These two special cases cover or, indeed, approximate

broad range of practically relevant situations including e.g. Gaussian distributions (reduce asymptotically to equidistribution in $B_n(1)$ for n large enough) and data vectors in which each attribute is a numerical and independent random variable.

Consider the case when the underlying probability distribution is an equidistribution in the unit ball $B_n(1)$, and suppose that $\mathcal{M} = \{\mathbf{x}_1, \dots, \mathbf{x}_M\}$ and $\mathcal{Y} = \{\mathbf{x}_{M+1}, \dots, \mathbf{x}_{M+k}\}$ are i.i.d. samples from this distribution. We are interested in determining the probability $\mathcal{P}_1(\mathcal{M}, \mathcal{Y})$ that there exists a linear functional l separating \mathcal{M} and \mathcal{Y} . An estimate of this probability is provided in the following theorem

Theorem 1. *Let $\mathcal{M} = \{\mathbf{x}_1, \dots, \mathbf{x}_M\}$ and $\mathcal{Y} = \{\mathbf{x}_{M+1}, \dots, \mathbf{x}_{M+k}\}$ be i.i.d. samples from the equidistribution in $B_n(1)$. Then*

$$\mathcal{P}_1(\mathcal{M}, \mathcal{Y}) \geq \max_{\delta, \varepsilon} (1 - (1 - \varepsilon)^n)^k \prod_{m=1}^{k-1} \left(1 - m(1 - \delta^2)^{\frac{m}{2}}\right) \left(1 - \frac{\Delta(\varepsilon, \delta, k)^{\frac{n}{2}}}{2}\right)^M$$

$$\Delta(\varepsilon, \delta, k) = 1 - \left[\frac{(1 - \varepsilon)\sqrt{1 - (k-1)\delta^2}}{\sqrt{k}} - (k-1)^{\frac{1}{2}}\delta \right]^2$$

Subject to :

$$\delta, \varepsilon \in (0, 1)$$

$$1 - (k-1)\delta^2 \geq 0$$

$$(k-1)(1 - \delta^2)^{\frac{n}{2}} \leq 1$$

$$\frac{(1 - \varepsilon)\sqrt{1 - (k-1)\delta^2}}{\sqrt{k}} - (k-1)^{\frac{1}{2}}\delta \geq 0.$$
(1)

Proof of Theorem 1. Given that elements in the set \mathcal{Y} are independent, the probability p_1 that $\mathcal{Y} \subset B_n(1) \setminus B_n(1 - \varepsilon)$ is

$$p_1 = (1 - (1 - \varepsilon)^n)^k.$$

Consider an auxiliary set

$$\hat{\mathcal{Y}} = \left\{ \hat{\mathbf{x}}_i \in \mathbb{R}^n \mid \hat{\mathbf{x}}_i = (1 - \varepsilon) \frac{\mathbf{x}_{M+i}}{\|\mathbf{x}_{M+i}\|}, i = 1, \dots, k \right\}.$$

Vectors $\hat{\mathbf{x}}_i \in \hat{\mathcal{Y}}$ belong to the sphere of radius $1 - \varepsilon$ centred at the origin (see Figure 1, (b)). According to [17] (proof of Proposition 3 and estimate (26)), the probability p_2 that for a given a given $\delta \in (0, 1)$ all elements of $\hat{\mathcal{Y}}$ are pair-wise $\delta/(1 - \varepsilon)$ -orthogonal, i.e.

$$|\cos(\hat{\mathbf{x}}_i, \hat{\mathbf{x}}_j)| \leq \frac{\delta}{1 - \varepsilon} \text{ for all } i, j \in \{1, \dots, k\}, i \neq j, \quad (2)$$

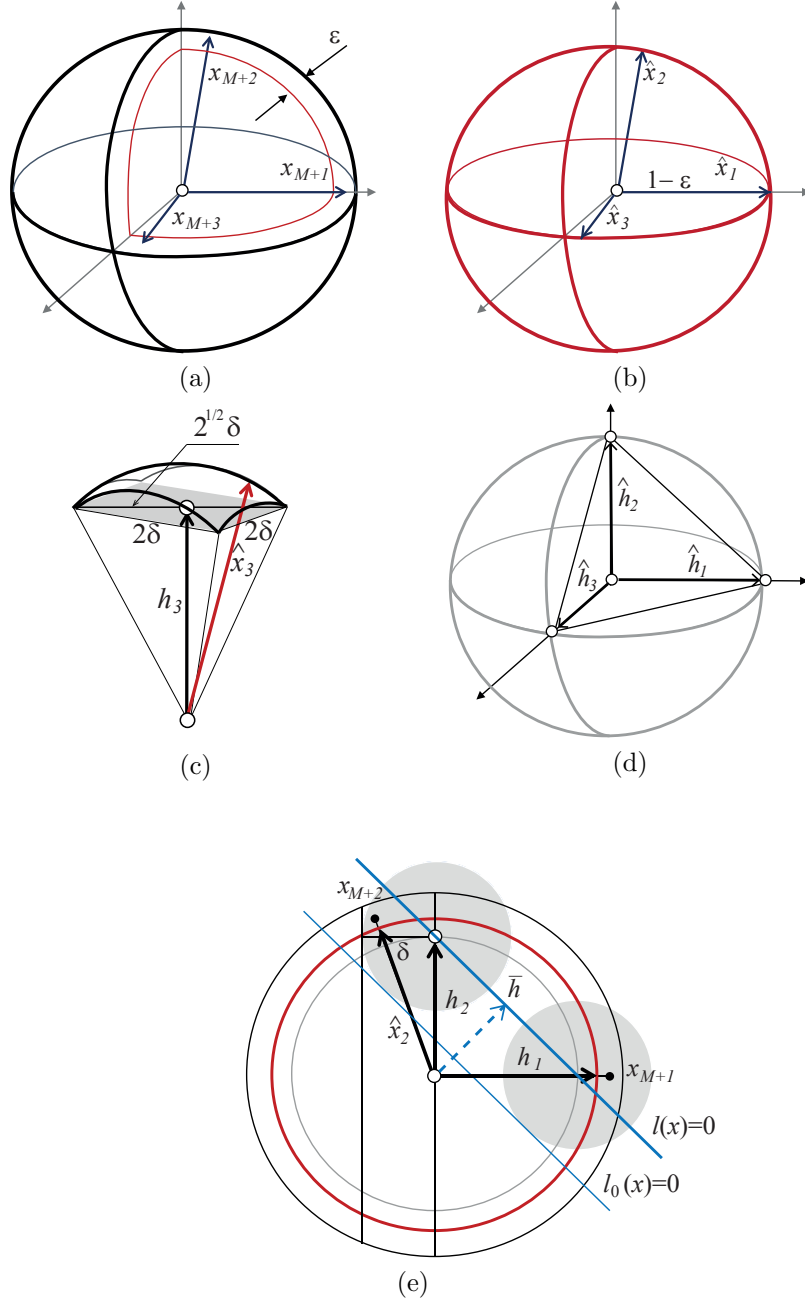


Figure 1: Illustration to the proof of Theorem 1. Panel (a) shows \mathbf{x}_{M+1} , \mathbf{x}_{M+2} and \mathbf{x}_{M+3} in the set $B_n(1) \setminus B_n(1 - \varepsilon)$. Panel (b) shows $\hat{\mathbf{x}}_1$, $\hat{\mathbf{x}}_2$, and $\hat{\mathbf{x}}_3$ on the sphere $S_{n-1}(1 - \varepsilon)$. Panel (c): construction of \mathbf{h}_3 . Note that $\|\mathbf{h}_3\| = \|\hat{\mathbf{x}}_3\|(1 - 2\delta^2)^{1/2} = (1 - \varepsilon)(1 - 2\delta^2)^{1/2}$. Panel (d) shows simplex formed by orthogonal vectors $\hat{\mathbf{h}}_1, \hat{\mathbf{h}}_2, \hat{\mathbf{h}}_3$. Panel (e) illustrates derivation of functionals l and l_0 .

can be estimated from below as:

$$p_2 \geq p_1 \prod_{m=1}^{k-1} \left(1 - m(1 - \delta^2)^{\frac{\alpha}{2}}\right) = (1 - (1 - \varepsilon)^n)^k \prod_{m=1}^{k-1} \left(1 - m(1 - \delta^2)^{\frac{\alpha}{2}}\right).$$

for $(k-1)(1 - \delta^2)^{\frac{\alpha}{2}} \leq 1$. Suppose now that (2) holds true. Let δ be chosen so that $1 - (k-1)\delta^2 \geq 0$. If this is the case than there exists a set of k pair-wise orthogonal vectors

$$\mathcal{H} = \{\mathbf{h}_1, \mathbf{h}_2, \dots, \mathbf{h}_k\}, \langle \mathbf{h}_i, \mathbf{h}_j \rangle = 0, \quad i, j \in \{1, \dots, k\}, \quad i \neq j,$$

such that (Figure 1, (c))

$$\|\hat{\mathbf{x}}_i - \mathbf{h}_i\| \leq (i-1)^{\frac{1}{2}}\delta, \quad \|\mathbf{h}_i\| = (1 - \varepsilon)(1 - (i-1)\delta^2)^{\frac{1}{2}}, \quad \text{for all } i \in \{1, \dots, k\}. \quad (3)$$

Finally, consider the set

$$\hat{\mathcal{H}} = \left\{ \hat{\mathbf{h}}_i \in \mathbb{R}^n \mid \hat{\mathbf{h}}_i = (1 - \varepsilon)(1 - (k-1)\delta^2)^{\frac{1}{2}} \frac{\mathbf{h}_i}{\|\mathbf{h}_i\|}, \quad i = 1, \dots, k \right\}$$

The set $\hat{\mathcal{H}}$ belongs to the sphere of radius $(1 - (k-1)\delta^2)^{\frac{1}{2}}$, and its k elements are vertices of the corresponding $k-1$ -simplex in \mathbb{R}^n (Figure 1, (d)).

Consider the functional:

$$l(\mathbf{x}) = \left\langle \frac{\bar{\mathbf{h}}}{\|\bar{\mathbf{h}}\|}, \mathbf{x} \right\rangle - \frac{(1 - \varepsilon)\sqrt{1 - (k-1)\delta^2}}{\sqrt{k}}, \quad \bar{\mathbf{h}} = \frac{1}{k} \sum_{i=1}^k \hat{\mathbf{h}}_i.$$

Recall that if $\mathbf{e}_1, \dots, \mathbf{e}_k$ are orthonormal vectors in \mathbb{R}^n then $\|\mathbf{e}_1 + \mathbf{e}_2 + \dots + \mathbf{e}_k\|^2 = k$. Hence $\left\| \sum_{i=1}^k \hat{\mathbf{h}}_i \right\| = \sqrt{k}(1 - \varepsilon)\sqrt{1 - (k-1)\delta^2}$, and we can conclude that $l(\hat{\mathbf{h}}_i) = 0$ and $l(\mathbf{h}_i) \geq 0$ for all $i = 1, \dots, k$. According to (3), $\|\hat{\mathbf{x}}_i - \mathbf{h}_i\| \leq (k-1)^{\frac{1}{2}}\delta$ for all $i = 1, \dots, k$. Therefore the functional

$$l_0(\mathbf{x}) = l(\mathbf{x}) + (k-1)^{\frac{1}{2}}\delta = \left\langle \frac{\bar{\mathbf{h}}}{\|\bar{\mathbf{h}}\|}, \mathbf{x} \right\rangle - \left(\frac{(1 - \varepsilon)\sqrt{1 - (k-1)\delta^2}}{\sqrt{k}} - (k-1)^{\frac{1}{2}}\delta \right) \quad (4)$$

satisfies the following condition: $l_0(\hat{\mathbf{x}}_i) \geq 0$ and $l_0(\mathbf{x}_{M+i}) \geq 0$ for all $i = 1, \dots, k$. This is illustrated with Figure 1, (e).

The functional l_0 partitions the unit ball $B_n(1)$ into the union of two disjoint sets: the spherical cap \mathcal{C}

$$\mathcal{C} = \{\mathbf{x} \in B_n(1) \mid l_0(\mathbf{x}) \geq 0\} \quad (5)$$

and its complement in $B_n(1)$, $B_n(1) \setminus \mathcal{C}$. The volume \mathcal{V} of the cap \mathcal{C} can be estimated from above as

$$\mathcal{V}(\mathcal{C}) \leq \frac{\Delta(\varepsilon, \delta, k)^{\frac{\alpha}{2}}}{2},$$

$$\Delta(\varepsilon, \delta, k) = 1 - \left[\frac{(1 - \varepsilon)\sqrt{1 - (k-1)\delta^2}}{\sqrt{k}} - (k-1)^{\frac{1}{2}}\delta \right]^2.$$

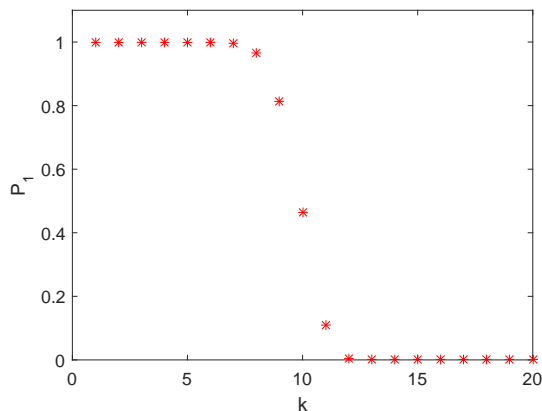


Figure 2: Estimate (1) of $\mathcal{P}_1(\mathcal{M}, \mathcal{Y})$ as a function of k for $n = 2000$ and $M = 10^5$.

Hence the probability p_3 that $l_0(\mathbf{x}_i) < 0$ for all $\mathbf{x}_i \in \mathcal{M}$ can be estimated from below as

$$p_3 \geq \left(1 - \frac{\Delta(\varepsilon, \delta, k)^{\frac{n}{2}}}{2}\right)^M.$$

Therefore, for fixed $\varepsilon, \delta \in (0, 1)$ chosen so that $\frac{(1-\varepsilon)\sqrt{1-(k-1)\delta^2}}{\sqrt{k}} - (k-1)^{\frac{1}{2}}\delta \geq 0$, the probability $p_4(\varepsilon, \delta)$ that \mathcal{M} can be separated from \mathcal{Y} by the functional l_0 can be estimated from below as:

$$p_4(\varepsilon, \delta) \geq (1 - (1 - \varepsilon)^n)^k \prod_{m=1}^{k-1} \left(1 - m(1 - \delta^2)^{\frac{n}{2}}\right) \left(1 - \frac{\Delta(\varepsilon, \delta, k)^{\frac{n}{2}}}{2}\right)^M.$$

Given that this estimate holds for all feasible values of ε, δ , statement (1) follows. \square

Figure 2 shows how estimate (1) of the probability $\mathcal{P}_1(\mathcal{M}, \mathcal{Y})$ behaves, as a function of $|\mathcal{Y}|$ for fixed M and n . As one can see from this figure, when k exceeds some critical value ($k = 9$ in this specific case), the lower bound estimate (1) of the probability $\mathcal{P}_1(\mathcal{M}, \mathcal{Y})$ drops. This is not surprising since the bound (1) is a) based on rough, L_∞ -like, estimates, and b) these estimates are derived for just one class of separating functionals $l_0(\mathbf{x})$. Furthermore, no prior preprocessing and/or clustering was assumed for the \mathcal{Y} . An alternative estimate that allows us to account for possible clustering in the set \mathcal{Y} is presented in Theorem 2.

Theorem 2. Let $\mathcal{M} = \{\mathbf{x}_1, \dots, \mathbf{x}_M\}$ and $\mathcal{Y} = \{\mathbf{x}_{M+1}, \dots, \mathbf{x}_{M+k}\}$ be *i.i.d.* samples from the equidistribution in $B_n(1)$. Let $\mathcal{Y}_c = \{\mathbf{x}_{M+r_1}, \dots, \mathbf{x}_{M+r_m}\}$ be a subset of m elements from \mathcal{Y} such that

$$\beta_2(m-1) \leq \sum_{r_j, r_j \neq r_i} \langle \mathbf{x}_{M+r_i}, \mathbf{x}_{M+r_j} \rangle \leq \beta_1(m-1) \text{ for all } i = 1, \dots, m. \quad (6)$$

Then

$$\mathcal{P}_1(\mathcal{M}, \mathcal{Y}_c) \geq \max_{\varepsilon \in (0,1)} (1 - (1 - \varepsilon)^n)^k \left(1 - \frac{\Delta(\varepsilon, m)^{\frac{n}{2}}}{2}\right)^M$$

$$\Delta(\varepsilon, m) = 1 - \frac{1}{m} \left(\frac{(1 - \varepsilon)^2 + \beta_2(m - 1)}{\sqrt{1 + (m - 1)\beta_1}} \right)^2 \quad (7)$$

Subject to :

$$(1 - \varepsilon)^2 + \beta_2(m - 1) > 0$$

$$1 + (m - 1)\beta_1 > 0.$$

Proof of Theorem 2. Consider the set \mathcal{Y} . Observe that $\|\mathbf{x}_{M+i}\| \geq 1 - \varepsilon$, $\varepsilon \in (0, 1)$, for all $i = 1, \dots, k$, with probability $p_1 = (1 - (1 - \varepsilon)^n)^k$. Consider now the vector $\bar{\mathbf{y}}$

$$\bar{\mathbf{y}} = \frac{1}{m} \sum_{i=1}^m \mathbf{x}_{M+r_i},$$

and evaluate the following inner products

$$\left\langle \frac{\bar{\mathbf{y}}}{\|\bar{\mathbf{y}}\|}, \mathbf{x}_{M+r_i} \right\rangle = \frac{1}{m\|\bar{\mathbf{y}}\|} \left(\langle \mathbf{x}_{M+r_i}, \mathbf{x}_{M+r_i} \rangle + \sum_{r_j, j \neq i} \langle \mathbf{x}_{M+r_i}, \mathbf{x}_{M+r_j} \rangle \right), \quad i = 1, \dots, m.$$

According to assumption (6), with probability p_1 ,

$$\left\langle \frac{\bar{\mathbf{y}}}{\|\bar{\mathbf{y}}\|}, \mathbf{x}_{M+r_i} \right\rangle \geq \frac{1}{m\|\bar{\mathbf{y}}\|} ((1 - \varepsilon)^2 + \beta_2(m - 1))$$

and, respectively,

$$\frac{1}{m} (1 + (m - 1)\beta_1) \geq \langle \bar{\mathbf{y}}, \bar{\mathbf{y}} \rangle \geq \frac{1}{m} ((1 - \varepsilon)^2 + \beta_2(m - 1))$$

Let $(1 - \varepsilon)^2 + \beta_2(m - 1) > 0$ and $(1 - \varepsilon)^2 + \beta_1(m - 1) > 0$. Consider the functional

$$l_0(\mathbf{x}) = \left\langle \frac{\bar{\mathbf{y}}}{\|\bar{\mathbf{y}}\|}, \mathbf{x} \right\rangle - \frac{1}{\sqrt{m}} \left(\frac{(1 - \varepsilon)^2 + \beta_2(m - 1)}{\sqrt{1 + (m - 1)\beta_1}} \right). \quad (8)$$

It is clear that $l_0(\mathbf{x}_{M+r_i}) \geq 0$ for all $i = 1, \dots, m$ by the way the functional is constructed. The functional $l_0(\mathbf{x})$ partitions the ball $B_n(1)$ into two sets: the set \mathcal{C} defined as in (5) and its complement, $B_n(1) \setminus \mathcal{C}$. The volume \mathcal{V} of the set \mathcal{C} is bounded from above as

$$\mathcal{V}(\mathcal{C}) \leq \frac{\Delta(\varepsilon, m)^{\frac{n}{2}}}{2}$$

where

$$\Delta(\varepsilon, m) = 1 - \frac{1}{m} \left(\frac{(1 - \varepsilon)^2 + \beta_2(m - 1)}{\sqrt{1 + \beta_1(m - 1)}} \right)^2.$$

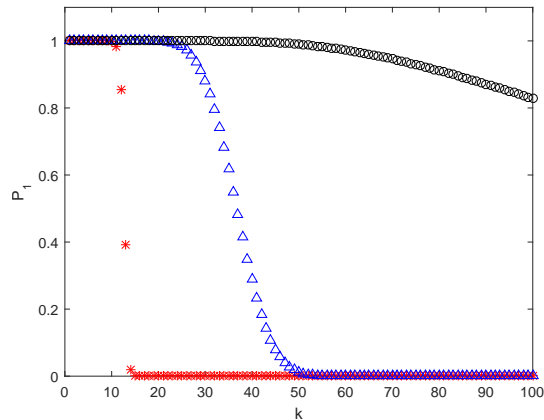


Figure 3: Estimate (7) of $\mathcal{P}_1(\mathcal{M}, \mathcal{Y})$ as a function of k for $n = 2000$ and $M = 10^5$. Red stars correspond to $\beta_1 = 0.5, \beta_2 = 0$. Blue triangles stand for $\beta_1 = 0.5, \beta_2 = 0.05$, and black circles stand for $\beta_1 = 0.5, \beta_2 = 0.07$.

Estimate (7) now follows. \square

Examples of estimates (7) for various parameter settings are shown in Fig. 3. As one can see, in absence of pair-wise strictly positive correlation assumption, $\beta_1 = 0$, the estimate's behavior, as a function of k , is similar to that of (1). However, presence of moderate pair-wise positive correlation results in significant boosts to the values of \mathcal{P}_1 .

Remark 1. Estimates (1), (7) for the probability $P_1(\mathcal{M}, \mathcal{Y})$ that follow from Theorems 1, 2 assume that the underlying probability distribution is an equidistribution in $B_n(1)$. They can, however, be generalized to equidistributions in ellipsoids and Gaussian distributions (cf. [18]).

Note that proofs of Theorems 1, 2 are constructive. Not only they provide estimates from below of the probability that two random i.i.d. drawn samples from $B_n(1)$ are linearly separable, but also they present the corresponding separating functionals explicitly as (4) and (8), respectively. The latter functionals are similar to Fisher linear discriminants. Whilst having explicit separation functionals is an obvious advantage from practical view point, the estimates that are associated with such functionals do not account for more flexible alternatives. In what follows we present a generalization of the above results that accounts for such a possibility as well as extends applicability of the approach to samples from product distributions. The results are provided in Theorem 3.

Theorem 3. Consider the linear space $E = \text{span}\{\mathbf{x}_j - \mathbf{x}_{M+1} \mid j = M + 2, \dots, M + k\}$, let the cardinality $|\mathcal{Y}| = k$ of the set \mathcal{Y} be smaller than n . Consider the quotient space \mathbb{R}^n/E . Let $Q(\mathbf{x})$ be a representation of $\mathbf{x} \in \mathbb{R}^n$ in \mathbb{R}^n/E , and let the coordinates of $Q(\mathbf{x}_i)$, $i = 1, \dots, M + 1$ be independent random variables i.i.d. sampled from a product distribution in a unit cube with

variances $\sigma_j > \sigma_0 > 0$, $1 \leq j \leq n - k + 1$. Then for

$$M \leq \frac{\vartheta}{3} \exp\left(\frac{(n - k + 1)\sigma_0^4}{2}\right) - 1$$

with probability $p > 1 - \vartheta$ there is a linear functional separating \mathcal{Y} and \mathcal{M} .

Proof of Theorem 3. Observe that, in the quotient space \mathbb{R}^n/E , elements of the set

$$\mathcal{Y} = \{\mathbf{x}_{M+1}, \mathbf{x}_{M+1} + (\mathbf{x}_{M+2} - \mathbf{x}_{M+1}), \dots, \mathbf{x}_{M+1} + (\mathbf{x}_{M+k} - \mathbf{x}_{M+1})\}$$

are vectors whose coordinates coincide with that of the quotient representation of \mathbf{x}_{M+1} . This means that the quotient representation of \mathcal{Y} consists of a single element, $Q(\mathbf{x}_{M+1})$. Furthermore, dimension of \mathbb{R}^n/E is $n - k + 1$. Let $R_0^2 = \sum_{i=1}^{n-k+1} \sigma_i^2$ and $\bar{Q}(\mathbf{x}) = \mathbb{E}(Q(\mathbf{x}))$. According to Theorem 2 and Corollary 2 from [16], for $\vartheta \in (0, 1)$ and M satisfying

$$M \leq \frac{\vartheta}{3} \exp\left(\frac{(n - k + 1)\sigma_0^4}{2}\right) - 1,$$

with probability $p > 1 - \vartheta$ the following inequalities hold:

$$\frac{1}{2} \leq \frac{\|Q(\mathbf{x}_j) - \bar{Q}(\mathbf{x})\|^2}{R_0^2} \leq \frac{3}{2}, \left\langle \frac{Q(\mathbf{x}_i) - \bar{Q}(\mathbf{x})}{R_0}, \frac{Q(\mathbf{x}_{M+1}) - \bar{Q}(\mathbf{x})}{\|Q(\mathbf{x}_{M+1}) - \bar{Q}(\mathbf{x})\|} \right\rangle < \frac{1}{\sqrt{2}}$$

for all i, j , $i \neq M + 1$. This implies that the functional

$$\ell_0(\mathbf{x}) = \left\langle \frac{Q(\mathbf{x}) - \bar{Q}(\mathbf{x})}{R_0}, \frac{Q(\mathbf{x}_{M+1}) - \bar{Q}(\mathbf{x})}{\|Q(\mathbf{x}_{M+1}) - \bar{Q}(\mathbf{x})\|} \right\rangle - \frac{1}{\sqrt{2}}$$

separates \mathcal{M} and \mathcal{Y} with probability $p > 1 - \vartheta$. \square

3. AI Knowledge Transfer Framework

In this section we show how Theorems 1, 2 and 3 can be applied for developing a novel one-shot AI knowledge transfer framework. We will focus on the case of transfer knowledge between two AI systems, a teacher AI and a student AI, in which input-output behaviour of the student AI is evaluated by the teacher AI. In this setting, assignment of AI roles, i.e. student or teaching, is beyond the scope of this manuscript. The roles are supposed to be pre-determined or otherwise chosen arbitrarily.

3.1. General setup

Consider two AI systems, a student AI, denoted as AI_s , and a teacher AI, denoted as AI_t . These legacy AI systems process some *input* signals, produce *internal* representations of the input and return some *outputs*. We further assume that some *relevant* information about the input, internal signals, and

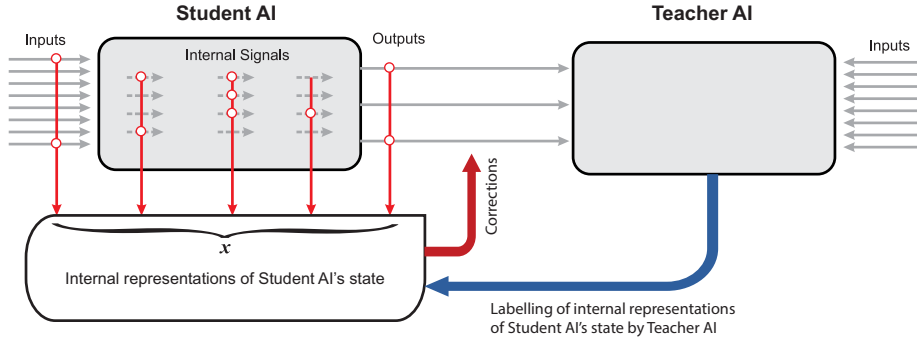


Figure 4: AI Knowledge transfer diagram. AI_s produces a set of its state representations, \mathcal{S} . The representations are labelled by AI_t into the set of correct responses, \mathcal{M} , and the set of errors, \mathcal{Y} . The student system, AI_s , is then augmented by an additional “corrector” eliminating these errors.

outputs of AI_s can be combined into a common object, \mathbf{x} , representing, but not necessarily defining, the *state* of AI_s . The objects \mathbf{x} are assumed to be elements of \mathbb{R}^n .

Over a period of activity system AI_s generates a set \mathcal{S} of objects \mathbf{x} . Exact composition of the set \mathcal{S} could depend on a task at hand. For example, if AI_s is an image classifier, we may be interested only in a particular subset of AI_s input-output data related to images of a certain known class. Relevant inputs and outputs of AI_s corresponding to objects in \mathcal{S} are then evaluated by the teacher, AI_t . If AI_s outputs differ to that of AI_t for the same input then an error is registered in the system. Objects $\mathbf{x} \in \mathcal{S}$ associated with errors are combined into the set \mathcal{Y} . The procedure gives rise to two disjoint sets:

$$\mathcal{M} = \mathcal{S} \setminus \mathcal{Y}, \quad \mathcal{M} = \{\mathbf{x}_1, \dots, \mathbf{x}_M\}$$

and

$$\mathcal{Y} = \{\mathbf{x}_{M+1}, \dots, \mathbf{x}_{M+k}\}.$$

A diagram schematically representing the process is shown in Fig. 4. The knowledge transfer task is to “teach” AI_s so that with

- a) AI_s does not make such errors
- b) existing competencies of AI_s on the set of inputs corresponding to internal states $\mathbf{x} \in \mathcal{M}$ are retained, and
- c) knowledge transfer from AI_t to AI_s is reversible in the sense that AI_s can “unlearn” new knowledge by modifying just a fraction of its parameters, if required.

Two algorithms for achieving such transfer knowledge are provided below.

3.2. Knowledge Transfer Algorithms

Our first algorithm, Algorithm 1, considers cases when *Auxiliary Knowledge Transfer Units*, i.e. functional additions to existing student AIs, are single linear functionals. The second algorithm, Algorithm 2, extends Auxiliary Knowledge Transfer Units to two-layer cascades of linear functionals.

The algorithms comprise of two general stages, pre-processing stage and knowledge transfer stage. The purpose of the pre-processing stage is to regularize and “sphere” the data. This operation brings the setup close to the one considered in statements of Theorems 1, 2. The knowledge transfer stage constructs Auxiliary Knowledge Transfer Units in a way that is very similar to the argument presented in the proofs of Theorems 1 and 2. Indeed, if $|\mathcal{Y}_{w,i}| \ll |\mathcal{S}_w \setminus \mathcal{Y}_{w,i}|$ then the term $(\text{Cov}(\mathcal{S}_w \setminus \mathcal{Y}_{w,i}) + \text{Cov}(\mathcal{Y}_{w,i}))^{-1}$ is close to identity matrix, and the functionals ℓ_i are good approximations of (8). In this setting, one might expect that performance of the knowledge transfer stage would be also closely aligned with the corresponding estimates (1), (7).

Remark 2. Note that the regularization step in the pre-processing stage ensures that the matrix $\text{Cov}(\mathcal{S}_w \setminus \mathcal{Y}_{w,i}) + \text{Cov}(\mathcal{Y}_{w,i})$ is non-singular. Indeed, consider

$$\begin{aligned} \text{Cov}(\mathcal{S}_w \setminus \mathcal{Y}_{w,i}) &= \frac{1}{|\mathcal{S}_w \setminus \mathcal{Y}_{w,i}|} \sum_{\mathbf{x} \in \mathcal{S}_w \setminus \mathcal{Y}_{w,i}} (\mathbf{x} - \bar{\mathbf{x}}(\mathcal{S}_w \setminus \mathcal{Y}_{w,i}))(\mathbf{x} - \bar{\mathbf{x}}(\mathcal{S}_w \setminus \mathcal{Y}_{w,i}))^T \\ &= \frac{1}{|\mathcal{S}_w \setminus \mathcal{Y}_{w,i}|} \left(\sum_{\mathbf{x} \in \mathcal{S}_w \setminus \mathcal{Y}_w} (\mathbf{x} - \bar{\mathbf{x}}(\mathcal{S}_w \setminus \mathcal{Y}_{w,i}))(\mathbf{x} - \bar{\mathbf{x}}(\mathcal{S}_w \setminus \mathcal{Y}_{w,i}))^T + \right. \\ &\quad \left. \sum_{\mathbf{x} \in \mathcal{Y}_w \setminus \mathcal{Y}_{w,i}} (\mathbf{x} - \bar{\mathbf{x}}(\mathcal{S}_w \setminus \mathcal{Y}_{w,i}))(\mathbf{x} - \bar{\mathbf{x}}(\mathcal{S}_w \setminus \mathcal{Y}_{w,i}))^T \right). \end{aligned}$$

Denoting $d = \bar{\mathbf{x}}(\mathcal{S}_w \setminus \mathcal{Y}_{w,i}) - \bar{\mathbf{x}}(\mathcal{S}_w \setminus \mathcal{Y}_w)$ and rearranging the sum below as

$$\begin{aligned} &\sum_{\mathbf{x} \in \mathcal{S}_w \setminus \mathcal{Y}_w} (\mathbf{x} - \bar{\mathbf{x}}(\mathcal{S}_w \setminus \mathcal{Y}_{w,i}))(\mathbf{x} - \bar{\mathbf{x}}(\mathcal{S}_w \setminus \mathcal{Y}_{w,i}))^T = \\ &\sum_{\mathbf{x} \in \mathcal{S}_w \setminus \mathcal{Y}_w} (\mathbf{x} - \bar{\mathbf{x}}(\mathcal{S}_w \setminus \mathcal{Y}_w) + d)(\mathbf{x} - \bar{\mathbf{x}}(\mathcal{S}_w \setminus \mathcal{Y}_w) + d)^T = \\ &\sum_{\mathbf{x} \in \mathcal{S}_w \setminus \mathcal{Y}_w} (\mathbf{x} - \bar{\mathbf{x}}(\mathcal{S}_w \setminus \mathcal{Y}_w))(\mathbf{x} - \bar{\mathbf{x}}(\mathcal{S}_w \setminus \mathcal{Y}_w))^T + \\ &2d \sum_{\mathbf{x} \in \mathcal{S}_w \setminus \mathcal{Y}_w} (\mathbf{x} - \bar{\mathbf{x}}(\mathcal{S}_w \setminus \mathcal{Y}_w))^T + |\mathcal{S}_w \setminus \mathcal{Y}_w| dd^T \\ &= \sum_{\mathbf{x} \in \mathcal{S}_w \setminus \mathcal{Y}_w} (\mathbf{x} - \bar{\mathbf{x}}(\mathcal{S}_w \setminus \mathcal{Y}_w))(\mathbf{x} - \bar{\mathbf{x}}(\mathcal{S}_w \setminus \mathcal{Y}_w))^T + |\mathcal{S}_w \setminus \mathcal{Y}_w| dd^T \end{aligned}$$

we obtain that $\text{Cov}(\mathcal{S}_w \setminus \mathcal{Y}_{w,i})$ is non-singular as long as the sum $\sum_{\mathbf{x} \in \mathcal{S}_w \setminus \mathcal{Y}_w} (\mathbf{x} - \bar{\mathbf{x}}(\mathcal{S}_w \setminus \mathcal{Y}_w))(\mathbf{x} - \bar{\mathbf{x}}(\mathcal{S}_w \setminus \mathcal{Y}_w))^T$ is non-singular. The latter property, however, is guaranteed by the regularization step in Algorithm 1.

Remark 3. Clustering at Step 2.a can be achieved by classical k -means algorithms [19] or any other method (see e.g. [20]) that would group elements of \mathcal{Y}_w into clusters according to spatial proximity.

Remark 4. Auxiliary Knowledge Transfer Units in Step 2.b of Algorithm 1 are derived in accordance with standard Fisher linear discriminant formalism. This, however, need not be the case, and other methods such as e.g. support vector machines [21] could be employed for this purpose there. It is worth mentioning, however, that support vector machines might be prone to overfitting

Algorithm 1 Single-functional AI Knowledge Transfer

1. Pre-processing

- (a) *Centering.* For the given set \mathcal{S} , determine the set average, $\bar{\mathbf{x}}(\mathcal{S})$, and generate sets \mathcal{S}_c

$$\begin{aligned}\mathcal{S}_c &= \{\mathbf{x} \in \mathbb{R}^n \mid \mathbf{x} = \boldsymbol{\xi} - \bar{\mathbf{x}}(\mathcal{S}), \boldsymbol{\xi} \in \mathcal{S}\}, \\ \mathcal{Y}_c &= \{\mathbf{x} \in \mathbb{R}^n \mid \mathbf{x} = \boldsymbol{\xi} - \bar{\mathbf{x}}(\mathcal{S}), \boldsymbol{\xi} \in \mathcal{Y}\}.\end{aligned}$$

- (b) *Regularization.* Determine covariance matrices $\text{Cov}(\mathcal{S}_c)$, $\text{Cov}(\mathcal{S}_c \setminus \mathcal{Y}_c)$ of the sets \mathcal{S}_c and $\mathcal{S}_c \setminus \mathcal{Y}_c$. Let $\lambda_i(\text{Cov}(\mathcal{S}_c))$, $\lambda_i(\text{Cov}(\mathcal{S}_c \setminus \mathcal{Y}_c))$ be their corresponding eigenvalues, and h_1, \dots, h_n be the eigenvectors of $\text{Cov}(\mathcal{S}_c)$. If some of $\lambda_i(\text{Cov}(\mathcal{S}_c))$, $\lambda_i(\text{Cov}(\mathcal{S}_c \setminus \mathcal{Y}_c))$ are zero or if the ratio $\frac{\max_i \{\lambda_i(\text{Cov}(\mathcal{S}_c))\}}{\min_i \{\lambda_i(\text{Cov}(\mathcal{S}_c))\}}$ is too large, project \mathcal{S}_c and \mathcal{Y}_c onto appropriately chosen set of $m < n$ eigenvectors, h_{n-m+1}, \dots, h_n :

$$\begin{aligned}\mathcal{S}_r &= \{\mathbf{x} \in \mathbb{R}^n \mid \mathbf{x} = H^T \boldsymbol{\xi}, \boldsymbol{\xi} \in \mathcal{S}_c\}, \\ \mathcal{Y}_r &= \{\mathbf{x} \in \mathbb{R}^n \mid \mathbf{x} = H^T \boldsymbol{\xi}, \boldsymbol{\xi} \in \mathcal{Y}_c\},\end{aligned}$$

where $H = (h_{n-m+1} \cdots h_n)$ is the matrix comprising of m significant principal components of \mathcal{S}_c .

- (c) *Whitening.* For the centered and regularized dataset \mathcal{S}_r , derive its covariance matrix, $\text{Cov}(\mathcal{S}_r)$, and generate whitened sets

$$\begin{aligned}\mathcal{S}_w &= \{\mathbf{x} \in \mathbb{R}^m \mid \mathbf{x} = \text{Cov}(\mathcal{S}_r)^{-\frac{1}{2}} \boldsymbol{\xi}, \boldsymbol{\xi} \in \mathcal{S}_r\}, \\ \mathcal{Y}_w &= \{\mathbf{x} \in \mathbb{R}^m \mid \mathbf{x} = \text{Cov}(\mathcal{S}_r)^{-\frac{1}{2}} \boldsymbol{\xi}, \boldsymbol{\xi} \in \mathcal{Y}_r\},\end{aligned}$$

2. Knowledge transfer

- (a) *Clustering.* Pick $p \geq 1$, $p \leq k$, $p \in \mathbb{N}$, and partition the set \mathcal{Y}_w into p clusters $\mathcal{Y}_{w,1}, \dots, \mathcal{Y}_{w,p}$ so that elements of these clusters are, on average, pairwise positively correlated. That is there are $\beta_1 \geq \beta_2 > 0$ such that:

$$\beta_2(|\mathcal{Y}_{w,i}| - 1) \leq \sum_{\boldsymbol{\xi} \in \mathcal{Y}_{w,i} \setminus \{\mathbf{x}\}} \langle \boldsymbol{\xi}, \mathbf{x} \rangle \leq \beta_1(|\mathcal{Y}_{w,i}| - 1) \text{ for any } \mathbf{x} \in \mathcal{Y}_{w,i}$$

- (b) *Construction of Auxiliary Knowledge Units.* For each cluster $\mathcal{Y}_{w,i}$, $i = 1, \dots, p$, construct separating linear functionals ℓ_i :

$$\begin{aligned}\ell_i(\mathbf{x}) &= \left\langle \frac{\mathbf{w}_i}{\|\mathbf{w}_i\|}, \mathbf{x} \right\rangle - c_i, \\ \mathbf{w}_i &= (\text{Cov}(\mathcal{S}_w \setminus \mathcal{Y}_{w,i}) + \text{Cov}(\mathcal{Y}_{w,i}))^{-1} (\bar{\mathbf{x}}(\mathcal{Y}_{w,i}) - \bar{\mathbf{x}}(\mathcal{S}_w \setminus \mathcal{Y}_{w,i}))\end{aligned}$$

where $\bar{\mathbf{x}}(\mathcal{Y}_{w,i})$, $\bar{\mathbf{x}}(\mathcal{S}_w \setminus \mathcal{Y}_{w,i})$ are the averages of $\mathcal{Y}_{w,i}$ and $\mathcal{S}_w \setminus \mathcal{Y}_{w,i}$, respectively, and c_i is chosen as $c_i = \min_{\boldsymbol{\xi} \in \mathcal{Y}_{w,i}} \left\langle \frac{\mathbf{w}_i}{\|\mathbf{w}_i\|}, \boldsymbol{\xi} \right\rangle$.

- (c) *Integration.* Integrate Auxiliary Knowledge Units into decision-making pathways of AIs. If, for an \mathbf{x} generated by an input to AIs, any of $\ell_i(\mathbf{x}) \geq 0$ then report \mathbf{x} accordingly (swap labels, report as an error etc.)
-

[22] and their training often involves iterative procedures such as e.g. sequential quadratic minimization [23].

Furthermore, instead of the sets $\mathcal{Y}_{w,i}$, $\mathcal{S}_w \setminus \mathcal{Y}_{w,i}$ one could use a somewhat more aggressive division: $\mathcal{Y}_{w,i}$ and $\mathcal{S}_w \setminus \mathcal{Y}_w$, respectively.

Depending on configuration of samples \mathcal{S} and \mathcal{Y} , Algorithm 1 may occasionally create knowledge transfer units, ℓ_i , that are “filtering” errors too aggressively. That is some $\mathbf{x} \in \mathcal{S}_w \setminus \mathcal{Y}_w$ may accidentally trigger non-negative response, $\ell_i(\mathbf{x}) \geq 0$, and as a result of this their corresponding inputs to A_s could be ignored or mishandled. To mitigate this, one can increase the number of clusters and knowledge transfer units, respectively. This will increase the probability of successful separation and hence alleviate the issue. On the other hand, if increasing the number of knowledge transfer units is not desirable for some reason, then two-functional units could be a feasible remedy. Algorithm 2 presents a procedure for such an improved AI Knowledge Transfer.

Algorithm 2 Two-functional AI Knowledge Transfer

1. **Pre-processing.** Do as in Step 1 in Algorithm 1
2. **Knowledge Transfer**
 - (a) *Clustering.* Do as in Step 2.a in Algorithm 1
 - (b) *Construction of Auxiliary Knowledge Units.*
 - 1: Do as in Step 2.b in Algorithm 1. At the end of this step *first-stage* functionals ℓ_i , $i = 1, \dots, p$ will be derived.
 - 2: For each set $\mathcal{Y}_{w,i}$, $i = 1, \dots, p$, evaluate the functionals ℓ_i for all $\mathbf{x} \in \mathcal{S}_w \setminus \mathcal{Y}_{w,i}$ and identify elements \mathbf{x} such that $\ell_i(\mathbf{x}) \geq 0$ and $\mathbf{x} \in \mathcal{S}_w \setminus \mathcal{Y}_w$ (incorrect error assignment). Let $\mathcal{Y}_{e,i}$ be the set containing such elements \mathbf{x} .
 - 3: **If** (there is an $i \in \{1, \dots, p\}$ such that $|\mathcal{Y}_{e,i}| + |\mathcal{Y}_{w,i}| > m$) **then** increment the value of p : $p \leftarrow p + 1$, and return to Step 2.a.
 - 4: **If** (all sets $\mathcal{Y}_{e,i}$ are empty) **then** proceed to Step 2.c.
 - 5: For each pair of ℓ_i and $\mathcal{Y}_{w,i} \cup \mathcal{Y}_{e,i}$ with $\mathcal{Y}_{e,i}$ not empty, project orthogonally sets $\mathcal{Y}_{w,i}$ and $\mathcal{Y}_{e,i}$ onto the hyperplane $\ell_i(\mathbf{x}) = 0$ and form the sets $\mathcal{L}_i(\mathcal{Y}_{w,i})$ and $\mathcal{L}_i(\mathcal{Y}_{e,i})$:

$$\begin{aligned} \mathcal{L}_i(\mathcal{Y}_{w,i}) &= \left\{ \mathbf{x} \in \mathbb{R}^m \mid \mathbf{x} = \left(I_m - \frac{\mathbf{w}_i \mathbf{w}_i^T}{\|\mathbf{w}_i\|^2} \right) \boldsymbol{\xi} + \frac{c_i \mathbf{w}_i}{\|\mathbf{w}_i\|}, \boldsymbol{\xi} \in \mathcal{Y}_{w,i} \right\}, \\ \mathcal{L}_i(\mathcal{Y}_{e,i}) &= \left\{ \mathbf{x} \in \mathbb{R}^m \mid \mathbf{x} = \left(I_m - \frac{\mathbf{w}_i \mathbf{w}_i^T}{\|\mathbf{w}_i\|^2} \right) \boldsymbol{\xi} + \frac{c_i \mathbf{w}_i}{\|\mathbf{w}_i\|}, \boldsymbol{\xi} \in \mathcal{Y}_{e,i} \right\}. \end{aligned}$$

- 6: Construct a linear functional $\ell_{2,i}$ separating $\mathcal{L}_i(\mathcal{Y}_{w,i})$ from $\mathcal{L}_i(\mathcal{Y}_{e,i})$ so that $\ell_{2,i}(\mathbf{x}) \geq 0$ for all $\mathbf{x} \in \mathcal{Y}_{w,i}$ and $\ell_{2,i}(\mathbf{x}) < 0$ for all $\mathbf{x} \in \mathcal{Y}_{e,i}$.
 - (c) *Integration.* Integrate Auxiliary Knowledge Units into decision-making pathways of AI_s . If, for an \mathbf{x} generated by an input to AI_s , any of the predicates $(\ell_i(\mathbf{x}) \geq 0) \wedge (\ell_{2,i}(\mathbf{x}) \geq 0)$ hold true then report \mathbf{x} accordingly (swap labels, report as an error etc.).
-

In what follows we illustrate the approach as well as the application of the proposed Knowledge Transfer algorithms in a relevant problem of a computer vision system design for pedestrian detection in live video streams.

4. Example

Let AI_s and AI_t be two systems developed, e.g. for the purposes of pedestrian detection in live video streams. Technological progress in embedded systems and availability of platforms such as e.g. Nvidia Jetson TX2 made hardware deployment of such AI systems at the edge of computer vision processing pipelines feasible. These AI systems, however, lack computational power to run state-of-the-art large scale object detection solutions such as e.g. ResNet [24] in real-time. Here we demonstrate that to compensate for this lack of power, AI Knowledge Transfer can be successfully employed. In particular, we suggest that the edge-based system is “taught” by the state-of-the-art teacher in a non-iterative and near-real time way. Since our building blocks are linear functionals, such learning will not lead to significant computational overheads. At the same time, as we will show later, the proposed AI Knowledge Transfer will result in a major boost to the system’s performance in the conditions of the experiment.

4.1. Definition of AI_s and AI_t and rationale

In our experiments, the teacher AI, AI_t , was modeled by a deep Convolutional Network, ResNet 18 [24] with circa 11M trainable parameters. The network was trained on a “teacher” dataset comprised of 5.2M non-pedestrian (negatives), and 600K pedestrian (positives) images. The student AI, AI_s , was modelled by a linear classifier with HOG features [25] and 2016 trainable parameters. The values of these parameters were the result of AI_s training on a “student” dataset, a sub-sample of the “teacher” dataset comprising of 55K positives and 130K negatives, respectively. This choice of AI_s and AI_t systems enabled us to emulate interaction between edge-based AIs and their more powerful counterparts that could be deployed on larger servers or computational clouds.

Moreover, to make the experiment more realistic, we assumed that internal states of both systems are inaccessible for direct observation. To generate sets \mathcal{S} and \mathcal{Y} required in Algorithms 1 and 2 we augmented system AI_s with an external generator of HOG features of the same dimension. We assumed, however, that covariance matrices of positives and negatives from the “student” dataset are available for the purposes of knowledge transfer. A diagram representing this setup is shown in Figure 5. A candidate image is evaluated by two systems simultaneously as well as by a HOG features generator. The latter generates 2016 dimensional vectors of HOGs and stores these vectors in the set \mathcal{S} . If outputs of AI_s and AI_t do not match the corresponding feature vector is added to the set \mathcal{Y} .

4.2. Error types

In this experiment we consider and address two types of errors: false positives (Type I errors) and false negatives (Type II errors). The error types were determined as follows. An error is deemed as *false positive* if AI_s reported presence of a correctly sized full-figure image of pedestrian in a given image

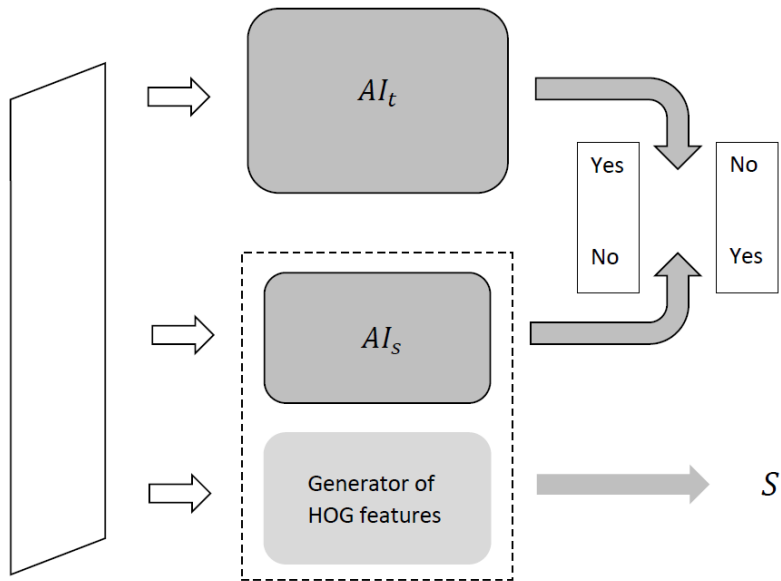


Figure 5: Knowledge transfer diagram between ResNet and HOG-SVM object detectors

patch whereas no such object was there. Similarly, an error is deemed as *false negative* if a pedestrian was present in the given image patch but AI_s did not report it there.

In our setting, evaluation of an image patch by AI_t (ResNet) took 0.01 sec on Nvidia K80 which was several orders slower than that of AI_s (linear HOG-based classifier). Whilst such behavior was expected, this imposed technical limitations on the process of mitigating errors of Type II. Each frame from our testing video produced 400K image patches to test. Evaluation of all these candidates by our chosen AI_t is prohibitive computationally. To overcome this technical difficulty we tested only a limited subset of image proposals with regards to these error type. To get a computationally viable number of proposals for false negative testing, we increased sensitivity of the HOG-based classifier by lowering its detection threshold from 0 to -0.3 . This way our linear classifier with lowered threshold acted as a filter letting through more true positives at the expense of large number of false positives. In this operational mode, Knowledge Transfer Unit were tasked to separate true positives from negatives in accordance with object labels supplied by AI_t .

4.3. Datasets

The approach was tested on two benchmark videos: LINTHESCHER sequence [26] created by ETHZ and comprised of 1208 frames and NOTTINGHAM video [27] containing 435 frames of live footage taken with an action camera. In what follows we will refer to these videos as ETHZ and NOTTINGHAM

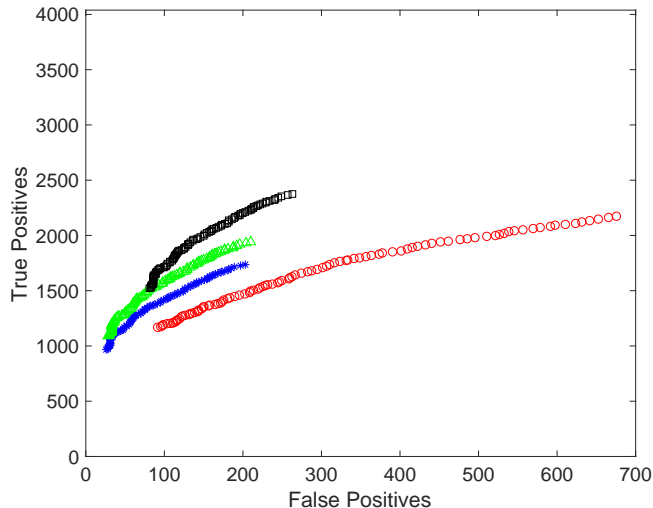


Figure 6: True positives as a function of false positives for NOTTINGHAM video.

videos, respectively. ETHZ video contains complete images of 8435 pedestrians, whereas NOTTINGHAM video has 4039 full-figure images of pedestrians.

4.4. Results

Performance and application of Algorithms 1, 2 for NOTTINGHAM and ETHZ videos are summarized in Fig. 6 and 7. Each curves in these figures is produced by varying the values of decision-making threshold in the HOG-based linear classifier. Red circles in Figure 6 show true positives as a function of false positives for the original linear classifier based on HOG features. Parameters of the classifier were set in accordance with Fisher linear discriminant formulae. Blue stars correspond to AI_s after Algorithm 1 was applied to mitigate errors of Type I in the system. The value of p (number of clusters) in the algorithm was set to be equal to 5. Green triangles illustrate application of Algorithm 2 for the same error type. Here Algorithm 2 was slightly modified so that the resulting Knowledge Transfer Unit had only one functional ℓ_2 . This was due to the low number of errors reaching stage two of the algorithm. Black squares correspond to AI_s after application of Algorithm 2 (error Type I) followed by application of Algorithm 2 to mitigate errors of Type II.

Figure 7 shows performance of the algorithms for ETHZ sequence. Red circles show performance of the original AI_s , green triangles correspond to AI_s supplemented with Knowledge Transfer Units derived using Algorithm 2 for errors of Type I. Black squares correspond to subsequent application of Algorithm 2 dealing with errors of Type II.

In all these cases, supplementing AI_s with Knowledge Transfer Units constructed with the help of Algorithms 1, 2 for both error types resulted in significant boost to AI_s performance. Observe that in both cases application of

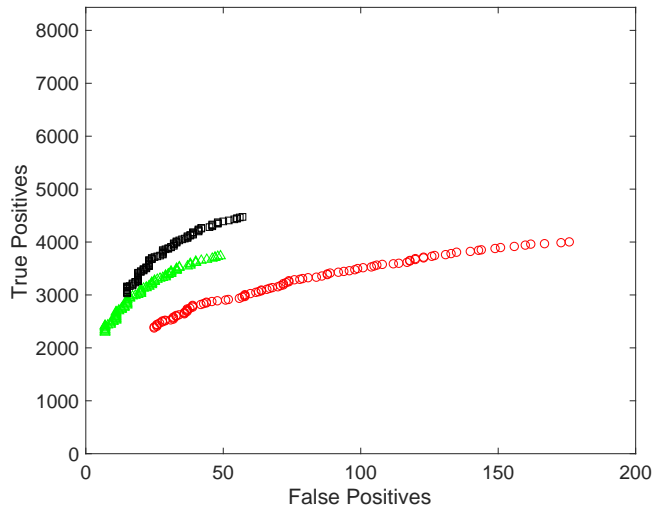


Figure 7: True positives as a function of false positives for ETHZ video.

Algorithm 2 to address errors of Type II has led to noticeable increases of numbers of false positives in the system at the beginning of the curves. Manual inspection of these false positives revealed that these errors are exclusively due mistakes of AI_t itself. For the sake of illustration, these errors for NOTTINGHAM video are shown in Fig. 8. These errors contain genuine false positives (images 12, 23-27) as well as mismatches by size (e.g. 1-7), and look-alikes (images 8,11,13,15-17).

5. Conclusion

In this work we proposed a framework for instantaneous knowledge transfer between AI systems whose internal state used for decision-making can be described by elements of a high-dimensional vector space. The framework enables development of non-iterative algorithms for knowledge spreading between legacy AI systems with heterogeneous non-identical architectures and varying computing capabilities. Feasibility of the framework was illustrated with an example of knowledge transfer between two AI systems for automated pedestrian detection in video streams.

In the basis of the proposed knowledge transfer framework are separation theorems (Theorem 1 – 3) stating peculiar properties of large but finite random samples in high dimension. According to these results, $k < n$ random i.i.d. elements can be separated from $M \gg n$ randomly selected elements i.i.d. sampled from the same distribution by few linear functionals, with high probability. The theorems are proved for equidistributions in a ball and in a cube. The results can be trivially generalized to equidistributions in ellipsoids and Gaussian distributions. Generalizations to other meaningful distributions is the subject of our future work.



Figure 8: False Positives induced by the teacher AI, AI_t .

Acknowledgments

The work was supported by Innovate UK Technology Strategy Board (Knowledge Transfer Partnership grants KTP009890 and KTP010522).

References

- [1] S. Gilev, A. Gorban, E. Mirkes, Small experts and internal conflicts in learning neural networks (malye eksperty i vnutrennie konflikty v obuchaemykh neironnykh setiakh), *Akademiia Nauk SSSR, Doklady* 320 (1) (1991) 220–223.
- [2] R. Jacobs, M. Jordan, S. Nowlan, G. Hinton, Adaptive mixtures of local experts, *Neural Computation* 3 (1) (1991) 79–87.
- [3] L. Pratt, Discriminability-based transfer between neural networks, *Advances in Neural Information Processing* (5) (1992) 204–211.
- [4] T. Schultz, F. Rivest, Knowledge-based cascade correlation, in: *Proceedings of the IEEE-INNS-ENNS International Joint Conference on Neural Networks*, IEEE, 2000, pp. 641–646.
- [5] J. Yosinski, J. Clune, Y. Bengio, H. Lipson, How transferable are features in deep neural networks?, in: *Advances in neural information processing systems*, 2014, pp. 3320–3328.
- [6] T. Chen, I. Goodfellow, J. Shlens, Net2net: Accelerating learning via knowledge transfer, *ICLR* 2016.
- [7] C. Bucila, R. Caruana, A. Niculescu-Mizil, Model compression, in: *KDD*, ACM, 2006, pp. 535–541. doi:10.1145/1150402.1150464.
- [8] G. Hinton, O. Vinyals, J. Dean, Distilling the knowledge in a neural network, cite arxiv:1503.02531Comment: NIPS 2014 Deep Learning Workshop (2015).
URL <http://arxiv.org/abs/1503.02531>
- [9] V. Vapnik, R. Izmailov, Knowledge transfer in svm and neural networks, *Annals of Mathematics and Artificial Intelligence* (2017) 1–17.
- [10] F. N. Iandola, S. Han, M. W. Moskewicz, K. Ashraf, W. J. Dally, K. Keutzer, Squeezenet: Alexnet-level accuracy with 50x fewer parameters and < 0.5mb model size, arXiv preprint, arXiv:1602.07360.
- [11] M. Gromov, *Metric Structures for Riemannian and non-Riemannian Spaces*. With appendices by M. Katz, P. Pansu, S. Semmes. Translated from the French by Sean Muchael Bates, Birkhauser, Boston, MA, 1999.
- [12] M. Gromov, Isoperimetry of waists and concentration of maps, *Gafa, Geometric and Functional Analysis* 13 (2003) 178–215.

- [13] J. Gibbs, Elementary Principles in Statistical Mechanics, developed with especial reference to the rational foundation of thermodynamics, Dover Publications, New York, 1960 [1902].
- [14] P. Lévy, Problèmes concrets d'analyse fonctionnelle, 2nd Edition, Gauthier-Villars, Paris, 1951.
- [15] A. Gorban, Order-disorder separation: Geometric revision, *Physica A* 374 (2007) 85–102.
- [16] A. Gorban, I. Tyukin, Stochastic separation theorems, *Neural Networks* 94 (2017) 255–259.
- [17] A. Gorban, I. Tyukin, D. Prokhorov, K. Soseikov, Approximation with random bases: Pro et contra, *Information Sciences* 364–365 (2016) 129–145.
- [18] A. Gorban, R. Burton, I. Romanenko, T. I., One-trial correction of legacy ai systems and stochastic separation theorems (11 2016).
URL <https://arxiv.org/abs/1610.00494>
- [19] S. P. Lloyd, Least squares quantization in pcm, *IEEE Transactions on Information Theory* 28 (2) (1982) 129–137.
- [20] R. Duda, P. Hart, D. Stork, *Pattern Classification*, Wiley, 2000.
- [21] V. Vapnik, *The Nature of Statistical Learning Theory*, Springer-Verlag, 2000.
- [22] H. Han, Analyzing support vector machine overfitting on microarray data, in: D. Huang, K. Han, M. Gromiha (Eds.), *Intelligent Computing in Bioinformatics. ICIC 2014. Lecture Notes in Computer Science*, Vol. 8590, Springer, Cham, 2014, pp. 148–156.
- [23] J. Platt, Sequential minimal optimization: A fast algorithm for training support vector machines, in: B. Schölkopf, C. Burges, A. Smola (Eds.), *Advances in Kernel Methods – Support Vector Learning*, MIT Press, Cambridge, 1998.
- [24] K. He, X. Zhang, S. Ren, J. Sun, Deep residual learning for image recognition, in: *2016 IEEE Conference on Computer Vision and Pattern Recognition*, 2016, pp. 770–778.
- [25] N. Dalal, B. Triggs, Histograms of oriented gradients for human detection, in: *Proc. of the IEEE Conference on Computer Vision and Pattern Recognition*, 2005, pp. 886–893.
- [26] A. Ess, B. Leibe, K. Schindler, L. van Gool, A mobile vision system for robust multi-person tracking, in: *Proc. of the IEEE Conference on Computer Vision and Pattern Recognition*, 2008, pp. 1–8, DOI: 10.1109/CVPR.2008.4587581.

- [27] R. Burton, Nottingham video, a test video for pedestrians detection taken from the streets of Nottingham by an action camera (2016).
URL <https://youtu.be/SJbh0JQCSuQ>